RESEARCH PAPERS

Nonlinear interactions between gravity waves and background winds*

Liu Xiao[1, 2**] and Xu Jiyao[1]

(1. State Key Laboratory for Space Weather, Center for Space Science and Applied Research, Chinese Academy of Sciences, Beijing 100080, China; 2. Graduate University of Chinese Academy of Sciences, Beijing 100039, China)

Accepted on October 23, 2006

Abstract Using the nonlinear propagating gravity waves (GW) model in the two-dimensional compressible atmosphere and the linear GW theory, the process of GW propagation in different background winds, e.g. the direction of the background wind is opposite to (dead wind) or the same as (tail wind) the direction of the horizontal phase velocity of GW, is studied. The results show that the dead wind prolongs the vertical wavelength and accelerates GW propagation. Therefore, GW propagates up to a higher height becomes instable in a short time and eventually induces an inverse jet flow. Then, the vertical wavelength is becoming short due to the nonlinear interactions between GW and the inverse jet flow. The vertical wavelength and group velocity decrease after GW propagates into the tail wind. The initial instable time is delayed. Although most of GW is trapped in the instable region, some of GW propagates above the instable region. Compared with GW propagation in the tail wind, the nonlinear interactions between GW and the dead wind are also strong. In contrast, the linear GW theory predicts that GW can propagate freely in the dead wind. The vertical wavelength simulated by the nonlinear numerical model is different from that predicted by the linear theory greatly after GW propagates into the dead wind.

Keywords: gravity waves, background winds, vertical group velocity, vertical wavelength, nonlinear interactions.

Recently, the theory of atmospheric dynamics and a mass of observations indicated that gravity wave (GW) plays an important role in the variations of the global atmospheric structures[1—4]. There are great differences between numerical simulations and observations of the dynamical structures of the global atmosphere if the effects of GW are neglected. Thus GW is important and indispensable to the process of atmospheric dynamics. Meanwhile, the dynamical structures of atmosphere have prominent influences on GW propagation. Because of the seasonal variations of the global atmospheric background winds, GW propagation in different background winds and its accelerated effects on the background winds are one of the hottest topics in atmospheric dynamics studies at present time[1—7].

GW propagation in the tail wind has received much attention and research[6, 7]. The reason is that the tail wind has obviously trapped and strong nonlinear effects on GW propagation.

GW can propagate freely in the dead wind in the classical linear GW theory. So the research about it is relatively poor. However, the observational results that the inverse jet flow occurring frequently in summer at middle latitudes are believed to be generated by breaking GW, which exerts a force on the dead winds through the deposition of their momentums and reverse the dead winds in the mesosphere[3, 4]. This indicates that the nonlinear interactions between GW and the dead winds are also strong. Thus further study is needed.

Very recently, we have developed a 2-dimensional numerical model to simulate the nonlinear propagating GW in the compressible atmosphere. The nonlinear interactions between photochemistry and dynamics during the process of GW propagation have been studied using this model[8, 9]. In this paper, we will study the nonlinear interactions between GW and background winds by using the model, especially, the effects of GW on the dead wind and the effects of the dead wind on the variations of GW propagation after

* Supported by National Natural Science Foundation of China (Grant Nos. 40225011, 40674088) and the National Program on Key Basic Research Projects (Grant No. 2006CB806306)

** To whom correspondence should be addressed. E-mail: xliu@spaceweather.ac.cn

GW propagates into the regions of the dead wind. For the purpose of comparative study, we will study the effects of GW on the tail wind and the effects of the tail wind on the variations of GW propagation after GW propagates into the regions of the tail wind. Firstly, we will analyze the effects of background winds on GW propagation based on the linear theory. Secondly, we will compare and study the nonlinear interactions (between GW and background wind) in the dead wind with that in the tail wind.

1 Linear theory of the effects of background winds on GW propagation

This section describes the study on the variations of GW propagation when GW packet propagates from the region without wind to the region with wind. For medium and small scale GW, the horizontal and vertical wavelengths used in this paper are 100 km and 10 km respectively. The wave period is 55.7 minutes. The vertical profiles of background winds are shown in Fig. 1(a). The solid and dash lines are the dead (Case 1) and tail wind (Case 2) respectively.

The effect of background winds on GW propagation is studied based on the ray tracing method and GW dispersion relation. The propagation characteristics, such as vertical group velocity and vertical wavelength, are important wave parameters. The following formula shows the relation between the vertical wave number and the vertical gradient of the background wind based on the ray tracing method[10],

$$\mathrm{d}k_z(z)/\mathrm{d}t = -k_x \mathrm{d}u_0(z)/\mathrm{d}z \qquad (1)$$

where k_x and k_z are the wave numbers in the horizontal and vertical directions respectively, u_0 is the background wind, t is time, z is height. For upward GW propagation in this study, the vertical wave number $k_z<0$. Thus the vertical wave number decreases with time evolution when $\mathrm{d}u_0(z)/\mathrm{d}z>0$. But the absolute value of the vertical wave number increases, as a result, the vertical wavelength decreases. On the contrary, the vertical wavelength increases with time evolution when $\mathrm{d}u_0(z)/\mathrm{d}z<0$.

In order to obtain the relation between the time and height of GW propagation, we introduce the vertical group velocity because formula (1) gives the relation between the time evolution of the vertical wave number and the vertical gradient of the background wind. Thus formula (1) can be written as

$$k_z(z) = \int_0^t [-k_x \mathrm{d}u_0(z)/\mathrm{d}z]\,\mathrm{d}t = \int_{z_0}^{z} -[1/c_{gz}(z')][k_x \mathrm{d}u_0(z')/\mathrm{d}z']\,\mathrm{d}z' \qquad (2)$$

where the vertical group velocity $c_{gz}(z)$ calculates from the linear GW dispersion relation[1]

$$c_{gz}(z) = \frac{-k_z(z)\hat{\omega}(z)}{[k_x^2 + k_z^2(z) + 1/(4H^2)]} \qquad (3)$$

and the intrinsic frequency $\hat{\omega}(z)$ satisfies[1]

$$\hat{\omega}(z) = \left[\frac{N^2 k_x^2}{k_x^2 + k_z^2(z) + 1/(4H^2)}\right]^{1/2} \qquad (4)$$

where $N^2 = \frac{g}{T}\left(\frac{\mathrm{d}T}{\mathrm{d}z} + \frac{g}{c_p}\right)$ is the square of buoyancy frequency, g is the acceleration due to gravity, T the temperature, c_p the specific heat at constant pressure, and H the scale height. The vertical profiles of the vertical wave number (or wavelength) and group velocity can be obtained by using Eqs. (2)—(4) in the stable initial background winds.

We calculate the effects of background winds on GW propagation using the method mentioned above. Fig. 1(b) and 1(c) show the vertical profiles of the vertical group velocity c_{gz} and wavelength L_z ($L_z = 2\pi/k_z$) respectively. These figures show that the vertical group velocity and wavelength increase after GW propagates into the dead wind (Case 1), this indicates that the GW is accelerated obviously after it propagates into the dead wind. The vertical group velocity and wavelength decrease greatly after GW propagates into the tail wind. Hence GW propagates upward very slowly after it propagates into the tail wind in the condition of Case 2. The result that the vertical wavelength decreases greatly indicates that GW is compressed greatly.

2 Nonlinear interactions between GW and background winds

GW propagation in atmosphere is a nonlinear process, so we will study the nonlinear interactions between GW and background winds using the nonlinear model[8]. The nonlinear propagation of GW in the background winds (Fig. 1(a)) will be discussed and compared with the results based on the linear theory.

2.1 GW nonlinear propagation model in 2-D compressible atmosphere

We have developed a nonlinear propagating GW model in two-dimensional compressible atmosphere in [8]. In order to avoid the effect of the upper bound-

ary on GW propagation, the vertical domain extends from the ground to 200 km, the horizontal width is 100 km. Compared with [8], the Rayleigh friction coefficient becomes

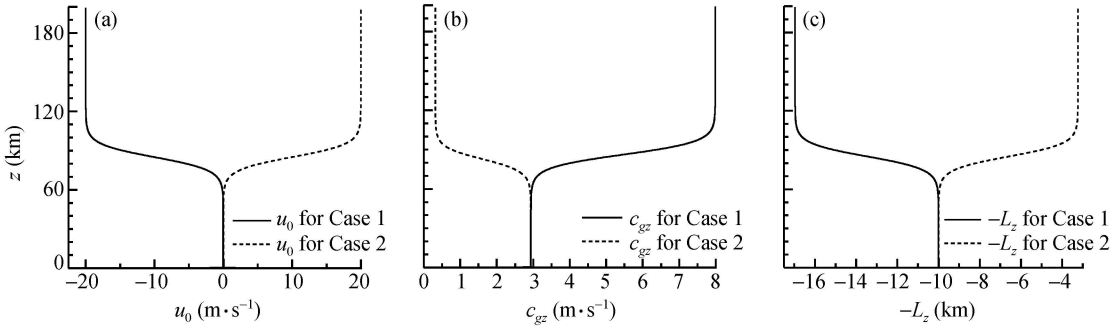

Fig. 1. The vertical profiles of background winds and wave parameters of Case 1 and Case 2. (a) Background winds; (b) vertical group velocity; (c) vertical wavelength.

$$\alpha(z)=\begin{cases}\alpha_0\exp\left[-\ln 2\cdot\left(\dfrac{z-180}{20}\right)\right], & z\leqslant 180\ \text{km}\\ \alpha_0, & z>180\ \text{km}\end{cases} \tag{5}$$

where $\alpha_0=0.02\ \text{s}^{-1}$. The Rayleigh friction provides a damping region near the top of the computational domain so that the wave reflections from the upper boundary can be eliminated greatly. Thus GW can propagate freely without any dissipation in a large height ranges.

2.2 The effects of background winds on GW propagation characteristics

In order to study the nonlinear GW propagation characteristics in the background winds shown in Fig. 1(a) and its accelerated effects on background winds, the amplitude of the initial horizontal velocity perturbation is taken as $3.0\ \text{m}\cdot\text{s}^{-1}$ in our numerical experiments. The horizontal and vertical wavelengths are 100 km and 10 km respectively. The other parameters are the same as that in [8]. Fig. 2 gives the spatial distribution of the potential temperature field (equal lines) and the convectively instable region ($N^2<0$, shadow) at two moments (shown at the right and top corner) in Case 1 (Fig. 2(a), (c)) and Case 2 (Fig. 2(b), (d)). Fig. 2 shows the same physical phenomena of the two cases because of the difference of the vertical group velocity between Case 1 and Case 2. Fig. 2(a), (b) show the moment that GW just become instable, and Fig. 2(c), (d) show the breaking GW for Case 1 and the instance at 15000s for Case 2.

Firstly, we analyze the effects of background winds on the height of the instable region. For Case 1 (Fig. 2(a), (c)), GW propagates to a higher height (120 km) in a short time (8400 s) due to the larger vertical group velocity in the dead wind. As a result, the amplitude of GW increases quickly and becomes convectively instable[11] because the density of atmosphere decreases exponentially with increasing height. For Case 2 (Fig. 2(b), (d)), the speed of the tail wind is smaller than the horizontal phase velocity of GW (that is, GW cannot reach the critical level), but there is a trapped effect on GW. The instable region is confined under 90 km, while the state of the region above 90 km is stable.

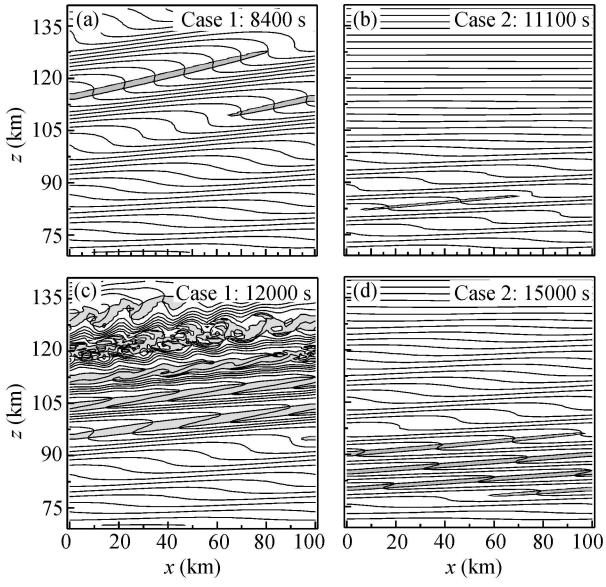

Fig. 2. The spatial distribution of potential temperature field (equal lines) and convectively instable region (shadow). (a) Initial instability occurring at 8400 s for Case 1; (b) initial instability occurring at 11000s for Case 2; (c) breaking occurring at 12000s for Case 1; (d) instable states at 15000s for Case 2.

Secondly, we analyze the effects of background winds on the initial instable time. For Case 1 (Fig. 2(a), (c)), GW becomes instable in a short time

(8400 s) due to the increase in the vertical group velocity of GW in the dead wind. On the other hand, according to Bretherton[12], the quantity $E/\hat{\omega}$ is conservative during GW propagation (E is the mean wave energy). The intrinsic frequency $\hat{\omega}$ increases with increasing height in the dead wind, thus GW extracts energy from the dead wind. The amplitude of GW is amplified due to the extracted energy and the decrease of the atmospheric density with height. As a result, GW becomes instable in a short time. At this height, GW transfers its energy to the background wind and results in an inverse jet flow (explanation in detail can be seen in Section 2.3). For Case 2, GW loses energy due to the intrinsic frequency $\hat{\omega}$ decreases with increasing height in the tail wind. Meanwhile, the upward propagation of GW is trapped because of the decrease of the vertical group velocity in the tail wind. Consequently, GW becomes instable after a long time.

Background winds have important effects on the vertical wavelength of GW based on the linear theory mentioned above. In order to study the effects of background winds on the vertical wavelength of GW based on the nonlinear numerical simulation, we present the time evolution of the normalized spectrum of the vertical wavelength of the horizontal velocity perturbation of GW in Case 1 (Fig. 3(a)) and Case 2 (Fig. 3(b)).

For Case 1, we find that the vertical wavelength of the horizontal velocity perturbation of GW is prolonged abruptly at about 4500 s. The reason is that the GW packet propagates into the region of the tail wind, the vertical wavelength is modulated by the dead wind and becoming longer until 8000 s. Then the sign of the vertical gradient of background wind is opposite to that in the initial time due to the accelerated effect of GW on the dead wind. So the vertical wavelength of GW is becoming short, GW begins to be instable and breaking above 95 km after 12000 s. These confine the increase of the amplitude of GW and excite waves with various wavelengths. Before 4500 s, there are few differences between the vertical wavelength simulated by the nonlinear numerical model and the one that is predicted by the linear theory (dash line). Then, the nonlinear interactions between GW and the dead wind are becoming strong with time evolution. Thus the vertical wavelengths simulated by the nonlinear numerical model are different from that predicted by the linear theory greatly. At 12000 s, the results of the nonlinear numerical simulation include several wavelengths. However, most of them (7.5 km and 10 km) are shorter than that predicted by the linear theory (about 16.5 km).

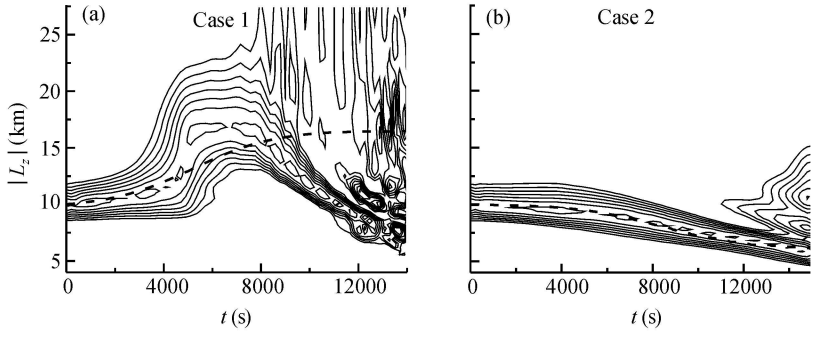

Fig. 3. The time evolution of the normalized spectrum of the vertical wavelength of the horizontal velocity perturbation of GW (equal line) and the vertical wavelength predicted by linear theory (dash line).

For Case 2, we find that the vertical wavelength is becoming short due to the modulation of the tail wind. Two different vertical wavelengths appear after 11000 s. They correspond to the regions above (stable region) and under (instable region) the height of 90 km (see Fig. 2). Furthermore, the vertical profiles of the horizontal velocity perturbation indicate that there are two parts of GW with different wavelengths above and under the height of 90 km (it is not shown in this paper). They correspond to the two main wavelengths shown in Fig. 3(b). The vertical wavelength of GW is compressed under the height of 90 km. Meanwhile, the vertical wavelength of GW is prolonged above the height of 90 km and GW propagates upward stably. The reason is that the tail wind extracts the energy of GW and the amplitude of GW decreases. The increase of the vertical wavelength of the upward propagating GW above the height of 90 km is in favor of GW propagation. The vertical wavelength simulated by the nonlinear numerical model co-

incides with that predicted by the linear theory before GW becomes instable (at about 11000 s). The vertical wavelength in Fig. 3(b) after 12000 s indicates that most of GW is confined into the instable region, but some of GW with longer vertical wavelength propagates stably above the instable region. It cannot be predicted by the linear theory.

The comparative results of Fig. 3(a) and 3(b) indicate that there are many differences between the vertical wavelength of GW simulated by the nonlinear numerical model and that predicted by the linear theory in the dead wind. However, the difference is small in the tail wind. These are caused by the inverse jet flow produced by the nonlinear interactions between GW and the dead wind. So there are many differences between the results of the nonlinear numerical simulation and that of the linear theory.

In a word, the dead (tail) wind accelerates (decelerates) the upward propagation and the development of the instability of GW during the initial stages of GW propagation. The vertical wavelength of GW is prolonged (compressed) when it propagates into the region of the dead (tail) wind. The vertical wavelength of GW simulated by the nonlinear numerical model is different from that predicted by the linear theory greatly due to the strong nonlinear interactions and the variations of background winds. GW accelerates the dead wind in the opposite direction at higher height when GW propagates into the region of the dead wind. The inverse jet flow (Section 2.3) traps the upward propagation of GW in the dead wind. Although the trapped effect of the tail wind on GW propagation, some of GW propagates upward freely in the tail wind.

2.3 The accelerated effects of GW on background winds

The accelerated effects of instable GW on background winds are one of the important aspects of wave-flow interactions[7, 13]. Thus here we study the variations of background winds due to GW propagation. The vertical profiles of background winds in Case 1 and Case 2 at several times are presented in Fig. 4 in which the propagation time is also shown.

GW propagates up to a higher height and becomes instable in a short time due to the accelerated effect of the dead wind on GW. As a result, the background wind is accelerated greatly. At 12000 s, the background wind with the initial speed -20 m·s^{-1} is accelerated to about 65 m·s^{-1} and an inverse jet flow appears at the height about 120 km. The sign of the vertical gradient of the background wind changes at about 7800 s and the vertical wavelength of GW decreases. This confirms the guess that the inverse jet flows occurring frequently in summer at middle latitudes are generated by breaking GW[4]. On the other hand, the inverse jet flow traps the upward propagation of GW and results in the complex structures of GW.

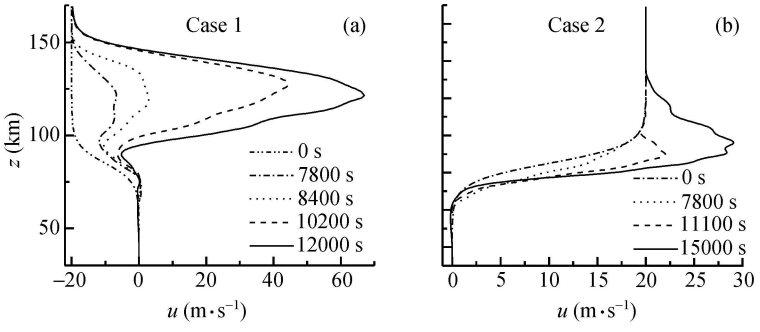

Fig. 4. The vertical profiles of horizontal background winds at several times.

Due to the trapped effect of the tail wind on the vertical wavelength and amplitude of GW, GW becomes instable in the region of the tail wind and this result in a relatively large acceleration of background wind at the bottom of the tail wind. Some of GW propagates upward from the region of the tail wind with time evolution. So the background wind is accelerated at the upper region of the tail wind and this results in a relatively weak jet flow.

The comparative results of Fig. 4(a) and 4(b) indicate that the magnitude of the acceleration of the background wind is large (small) and the height of the acceleration is high (low) when GW propagates into the region of the dead (tail) wind. These are caused by the accelerated effect of the dead wind on

GW, GW propagates to a higher height and deposit momentums in the instable region in a short time. Then, the deposited momentums induce an inverse jet flow. On the other hand, the inverse jet flow traps GW propagation in the dead wind.

3 Conclusions

In this paper, firstly, we analyze the effects of background winds on GW propagation by using the ray tracing method and the linear GW dispersion relation. The results indicate that the vertical group velocity and wavelength of GW increase (decrease) after GW propagates into the region of the dead (tail) wind. Secondly, we study the nonlinear propagation of GW in the dead (tail) wind by using the nonlinear propagating GW model[8] and compare them with that of the linear theory.

GW becomes instable quickly at a higher height due to the accelerated effect of the dead wind. The dead wind prolongs the vertical wavelength of GW. The instable GW induces the acceleration of the background wind and an inverse jet flow appears. This result confirms the guess in [4]. The new background wind shortens the vertical wavelength of GW gradually and traps the upward propagation and the amplitude of GW. The waves with different vertical wavelengths appear during the process of the nonlinear numerical simulation and different from that of the linear theory greatly. The initial instable time is delayed due to the trapped effect of the tail wind on GW. The vertical wavelength of GW is becoming short. GW becomes instable in the region of the tail wind. Although most of GW is trapped in the region of the tail wind, Some of GW propagates upward freely and stably above the instable region.

The magnitude and height of the accelerated effect of GW on background winds are related to the height of GW propagation directly. Hence, they are also related to the vertical group velocity. GW propagates to a higher height and extracts energy form the dead wind due to the accelerated effect of the dead wind on GW. So the background wind is accelerated greatly at a higher height and an inverse jet flow appears. On the contrary, the tail wind confines the vertical group velocity and the height of GW propagation, and extracts energy from GW. Consequently, the amplitude of GW increases slowly and the acceleration of the background wind is relatively small.

The simulative and comparative studies in this paper indicate that, compared with GW propagation in the tail wind, the nonlinear interactions between GW and the dead wind are also strong. There are large variations of GW propagation and the structures of the background wind. The vertical wavelength of GW simulated by the nonlinear numerical model is different from that of the linear theory greatly.

References

1 Fritts DC and Alexander MJ. Gravity wave dynamics and effects in the middle atmosphere. Rev Geophys, 2003, 41(1): 3-1—3-64

2 Goya K and Miyahara S. Non-hydrostatic nonlinear 2-D model simulations of internal gravity waves in realistic zonal winds. Adv Space Res, 1999, 24(11): 1523—1526

3 McLandress C. On the importance of gravity waves in the middle atmosphere and their parameterization in general circulation models. J Atmos Sol Terr Phys, 1998, 60(14): 1357—1383

4 Zhang SP and Shepherd GG. Variation of the mean winds and diurnal tides in the mesosphere and lower thermosphere observed by WINDII from 1992 to 1996. Geophys Res Lett, 2005, 32: L14111

5 Ding F, Wan W and Yuan H. The influence of background winds and attenuation on the propagation of atmospheric gravity waves. J Atmos Sol Terr Phys, 2003, 65(7): 857—869

6 Zhang SD, Yi F and Wang JF. The nonlinear propagation of gravity wave packet in the sheared ambient. Chinese Journal of Space Science (in Chinese), 1999, 19(2): 122—127

7 Fritts DC and Dunkerton TJ. A quasi-linear study of gravity wave saturation and self-acceleration. J Atmos Sci, 1984, 41: 3272—3289

8 Xu JY, Smith AK and Ma RP. A numerical study of the effect of gravity-wave propagation on minor species distributions in the mesopause region. J Geophys Res, 2003, 108(D3): 4119

9 Xu JY and Smith AK. Study of gravity wave-induced fluctuations of the sodium layer using linear and nonlinear models. J Geophys Res, 2004, 109: D02306

10 Jones WL. Ray tracing for internal gravity waves. J Geophys Res, 1969, 74(8): 2028—2033

11 Fritts DC. Gravity wave saturation in the middle atmosphere: a review of theory and observations. Rev Geophys, 1984, 22(3): 275—308

12 Bretherton FP. The propagation of groups of internal gravity waves in a shear flow. Q J R Meteorol Soc, 1966, 92: 466—480

13 Liu HL, Hays PB and Roble RG. A numerical study of gravity wave breaking and impacts on turbulence and mean state. J Atmos Sci, 1999, 56: 2152—2177